

气固两相透平内颗粒湍流扩散的 Lagarange 数值模拟

鲁嘉华, 凌志光

(上海工程技术大学 航空运输学院, 上海 200336)

摘要: 在双级跨音速燃气透平全三维黏性湍流场下, 采用气固双向耦合模型分别对不同粒度的煤颗粒以及体积分数为 $0.903 \times 10^{-4} \%$ 的 $5 \sim 50 \mu\text{m}$ 分布直径混合颗粒群在叶片流道内的湍流扩散运动进行了 Lagarange 数值模拟, 分别得到和分析了相应的运动轨迹和运动滑移。与无黏、层流、单向耦合假设条件下的数值模拟结果比较, 得到了颗粒真实的运动特性, 特别是在叶片根部、顶部和压力面上, 颗粒与叶片撞击点的分布与实际叶片冲蚀点分布情况较为吻合, 证实了叶片流道内颗粒湍流扩散特性的不可忽略性。数值模拟结果将为进一步优化气固两相透平叶片的气动设计提供更为可靠的依据。

关键词: 气固两相透平; 黏性湍流场; 湍流扩散; 双向耦合; Lagarange 法; 数值模拟

中图分类号: TK472 文献标识码: A

1 引言

气固两相透平在西气东输系统和增压流化床等装置中应用较广, 对叶片流道内颗粒运动的准确数值模拟, 可以为叶片气动设计的优化, 提高叶片的抗冲蚀能力提供科学依据。已有研究成果中, 有过分夸大颗粒在叶片子午面内向叶顶流动的趋势, 难以解释实际燃气轮机透平叶片根部由于颗粒冲蚀而导致的严重的型线破坏, 主要原因是简化了流场的复杂性所致^[1~3]。

Hiroyuki 等人的实验研究表明^[3], 颗粒浓度及粒度的不同, 都会引起流场湍流度的变化, 对分离以后进入叶片流道的微小颗粒, 继而又对流场有较大作用, 同时由于惯性, 流体与颗粒之间的运动滑移又凸现了流体的黏性效应。颗粒冲击壁面, 不仅冲蚀叶片、机匣, 还将影响颗粒此后的轨迹、在流场中的再分布以及后续对壁面的碰撞, 因此数值模拟更关心颗粒的历史流程。基于这些事实, 本文采用了 Euler-Lagarange 坐标下计入气固双向耦合和流场黏性及

颗粒随机轨道模型, 对叶片流道内颗粒运动特性进行了数值模拟, 经与简化模型的计算结果以及实物叶片的冲蚀现象比较后, 确认了本文模型的合理性。

2 气相湍流场数值模拟的模型

采用 Berlemont 等人提出的模型对气相湍流场进行模拟^[4], 为了顾及气相与颗粒间相互作用, 在动量方程、 k 方程和 ϵ 方程中, 加上颗粒源相。基本方程如式(1)~式(7)。

$$\text{连续方程: } \frac{\partial \rho u_i}{\partial x_i} = 0 \quad (1)$$

湍流动量方程:

$$\frac{\partial}{\partial x_i} (\rho u_i u_j) = - \frac{\partial}{\partial x_j} \left(p + \frac{2}{3} \rho k \right) - \frac{\partial}{\partial x_j} \times \left[\frac{2}{3} (\mu + \mu_t) \frac{\partial u_j}{\partial x_j} \right] + \frac{\partial}{\partial x_j} (\mu + \mu_t) \left(\frac{\partial u_i}{\partial x_j} + \frac{\partial u_j}{\partial x_i} \right) + S_{mi} \quad (2)$$

式(1)和式(2)中, ρ 为气体密度, u_i 为气体时均速度, p 为压力, k 为湍动能, μ 为流体动力黏性系数, μ_t 为湍流动力黏性系数, S_{mi} 为两相间动量交换引起的源相。若有 n 个颗粒轨道穿过计算单元, 其中第 j 个轨道含 n_j 个质量为 m_{pj} 的颗粒, 则所有轨道在某单元内流下的颗粒动量源项为:

$$S_{mi} = \left\{ \sum_{j=1}^n [n_j m_{pj} (u_{pj, \text{out}} - u_{pj, \text{in}})] \right\}_i \quad (3)$$

式中: $u_{pj, \text{out}}$ 、 $u_{pj, \text{in}}$ 是颗粒离开和进入计算单元时的速度值。

湍动能方程:

$$\frac{\partial}{\partial x_j} (\rho u_j k) = \frac{\partial}{\partial x_j} \left(\frac{\mu_t}{\sigma_k} \frac{\partial k}{\partial x_j} \right) + (G_k - \rho \epsilon + S_k) \quad (4)$$

式中: $\sigma_k = 1.0$, 为湍动能计算常数; ϵ 为湍动能耗散率; $G_k = \mu_t \frac{\partial u_i}{\partial x_j} \left(\frac{\partial u_i}{\partial x_j} + \frac{\partial u_j}{\partial x_i} \right)$ 为湍动能生成项; S_k 是

收稿日期: 2002-11-11; 修订日期: 2002-12-26

基金项目: 上海市教委科技发展基金资助项目(2000E12)

作者简介: 鲁嘉华(1960-)男, 上海人, 上海工程技术大学副教授, 工学博士。

颗粒存在引起的气体相湍动能源项, 表示为:

$$S_k = S_{mj} u_j \quad (5)$$

湍流能量耗散率方程为:

$$\frac{\partial}{\partial x_j} (\rho u_j \epsilon) = \frac{\partial}{\partial x_j} \left(\frac{\mu_t}{\sigma_\epsilon} \frac{\partial \epsilon}{\partial x_j} \right) + \left(C_1 \frac{\epsilon G_k}{k} - C_2 \rho \frac{\epsilon^2}{k} + S_\epsilon \right) \quad (6)$$

式中: C_1 、 C_2 、 C_3 为计算常数, 分别取值 $C_1 = 1.56$, $C_2 = 1.92$, $C_3 = 1.1$; S_ϵ 是颗粒存在引起的气相湍流能量耗散率源项, 表示为:

$$S_\epsilon = C_3 \frac{\epsilon}{k} S_k \quad (7)$$

3 气相流场的边界条件与初始条件

3.1 固体壁面

在叶片壁面、轮毂及机匣处, 黏性起主要作用, 湍流流动应满足无滑移条件。由于 $k-\epsilon$ 模型只适用于充分发展的高雷诺数湍流区域, 故采取了壁面函数法, 用相对较粗的网格得到黏性流场解。壁面函数法得到壁面到湍流核心区之间的流速 u_i 、 k 和 ϵ 的分布规律, 既节省计算机内存和机时, 又兼顾了壁面粗糙度的影响, 表示为:

$$\frac{u_{ps}}{u_\tau} = \frac{1}{k} \ln(Ey^+)$$

其中: $u_\tau = \frac{\tau_w}{\rho}$ 为壁面摩擦速度, τ_w 为壁面上的切应力; u_{ps} 为切向速度; $y^+ = \frac{y u_\tau}{\nu}$ 为无量纲摩擦长度, y 为计算区域内某点到壁面的距离; $\kappa = 0.435$ 是卡门常数; E 是粗糙度系数, 对光滑壁面 $E = 9.0$ 。在 $30 < y^+ < 100$ 范围内, 壁面函数构成了壁面上的全部边界条件。对运动壁面, u_{ps} 应改为 $u'_{ps} = |u_b - u_{ps}|$, 式中 u_b 为壁面的速度。

3.2 叶片排进口和出口处

叶片排进口处除了总温、总压和入口马赫数, k 、 ϵ 值未知, 因此可参考类似流场的取法给定 k 、 ϵ 入口值, 或通过试验来决定其值。根据 Spalding^[3] 建议, 最简单的方法是假定叶片排入口 k 和 ϵ 是均匀的, 由公式估算: $\sqrt{\frac{k}{U_\infty}} = I$; $\epsilon = C_\mu^{\frac{3}{4}} \frac{k^{\frac{3}{2}}}{l_m}$, I 是湍流强度(最常用值: $0.01 < I < 0.05$), $C_\mu = 0.09$, $l_m \approx 0.1H$, 这里 H 是入口特征长度, 如叶片高度。

出口断面上, 给出叶片静压, 还假定沿断面外法线 n 方向 k 、 ϵ 不再变化, 即 $\frac{\partial k}{\partial n} = 0$, $\frac{\partial \epsilon}{\partial n} = 0$ 。湍流场

计算中, 出口断面向下游延伸 1 ~ 2 个叶片弦长距离。

3.3 周期性边界条件

在周期性边界上相应点上的所有变量都相等, 即 $u_{r左} = u_{r右}$, $p_{左} = p_{右}$; $u_{\theta左} = u_{\theta右}$, $k_{左} = k_{右}$; $u_{z左} = u_{z右}$, $\epsilon_{左} = \epsilon_{右}$ 。

4 湍流扩散颗粒运动方程

颗粒运动转动圆柱坐标系 (r, θ, z) 系下, 具有湍流扩散的颗粒运动用随机轨道模型表达:

$$\begin{aligned} \ddot{r} &= B(\bar{u}_{gr} + u'_{gr} - u_{pr}) + g + \frac{1}{\rho_p} \frac{\partial p}{\partial r} + r(\dot{\vartheta} + \omega)^2 \\ \ddot{\vartheta} &= \frac{B}{r}(\bar{u}_{g\theta} + u'_{g\theta} - u_{p\theta}) + \frac{1}{r^2 \rho_p} \frac{\partial p}{\partial \vartheta} - \frac{2}{r} \dot{r}(\dot{\vartheta} + \omega) \\ \ddot{z} &= B(\bar{u}_{gz} + u'_{gz} - u_{pz}) + \frac{1}{\rho_p} \frac{\partial p}{\partial z} \end{aligned} \quad (8)$$

式中: $B = \frac{18 \mu_g f(Re_p)}{d_p^2 \rho_p}$, Re_p 为颗粒雷诺数; \bar{u}_g 、 $\bar{u}_{g\theta}$ 、 $\bar{u}_{g\theta}$ 为气相湍流流场平均速度; u_{pz} 、 u_{pr} 、 $u_{p\theta}$ 为颗粒速度分量; u'_{gr} 、 $u'_{g\theta}$ 、 $u'_{g\theta}$ 为气体脉动速度; ρ_p 为颗粒密度; μ_g 为气体动力黏性系数; d_p 是颗粒直径。脉动速度场的求解见文献[6 ~ 7]。

4.1 颗粒初始与边界条件

求解颗粒运动轨迹时, 在起始点需要给出颗粒的三个初始位置坐标及三个初始速度分量。本模拟中, 在第一排叶片进口处, 颗粒的初始位置 r 向和 ϑ 向坐标随机给定, 三个速度分量按如下方式确定 $u_{pz0} = \frac{dz}{dt} \Big|_{t=t_0} = F(d_p) u_{gz}$, $u_{pr0} = \frac{dr}{dt} \Big|_{t=t_0} = F(d_p) u_{gr}$, $u_{p\theta 0} = \frac{d\vartheta}{dt} \Big|_{t=t_0} = F(d_p) u_{g\theta}$ 。其中 u_{gz} 、 u_{gr} 、 $u_{g\theta}$ 为颗粒的初始位置上的气体速度分量, $F(d_p)$ 为速度滑移因子, 是一个与颗粒直径大小成反向变化的代数函数, 取值范围为 0 ~ 1.0。原则上, 颗粒直径愈大, 与气体的速度滑移愈明显, 故 $F(d_p)$ 取较小值; 反之 $F(d_p)$ 取较大值。以后各排叶片进口处, 颗粒初始位置的 r 向坐标根据前排叶片出口处的 r 向坐标确定, ϑ 坐标仍随机给定; 初始速度分量根据前排叶片出口处颗粒的速度分量经考虑动静叶之间关系的转换后给出。

Tabakoff 经回归分析^[4], 拟合出半经验型冲击反弹参数关系式和冲蚀率计算公式。有关冲击反弹

参数关系式一般表达式为 $e_t = u_{pt2}/u_{pt1} = A_0 + A_1\beta_1 + A_2\beta_1^2 + A_3\beta_1^3 + A_4\beta_1^4$, $e_n = u_{pn2}/u_{pn1} = B_0 + B_1\beta_1 + B_2\beta_1^2 + B_3\beta_1^3 + B_4\beta_1^4$, $\text{tg}\beta_2 = u_{pn2}/u_{pt2}$, $u_{p2} = \sqrt{u_{pn2}^2 + u_{pt2}^2}$, 式中: $A_0, A_1, A_2, A_3, A_4, B_0, B_1, B_2, B_3, B_4$ 均为试验常数; e_t, e_n 分别为切向和法向恢复系数; u_{p1} 和 u_{p2} 分别为颗粒碰撞固壁前后的速度, u_{pn1}, u_{pn2} 分别为颗粒碰撞固壁前后的法向分速度, u_{pt1}, u_{pt2} 分别为颗粒碰撞固壁前后的切向分速度; β_1, β_2 分别为颗粒的入射角和反弹角。

4.2 颗粒运动方程求解

颗粒运动方程的数值积分步骤为: 确定 Lagarange 时间步长, 该步长根据穿越单元的最短时间确定, 它与最小单元尺寸和最大颗粒速度分量有关; 移动颗粒到新的坐标, 新的颗粒位置通过积分方程 $\frac{dx_p}{dt} = \vec{u}_p$ 得到, 即 $x_p^n = x_p^0 + \vec{u}_p^0 \Delta t$, 其中 n 代表时间步长结束时的值, 0 代表时间步长开始时的值, Δt 为 Lagarange 时间步长。颗粒在每一时间步长内, 可以抵达下一单元, 但不允许跳跃相邻的单元。在壁面边界, 通过调整时间步长, 将颗粒置于边界单元内; 计算新坐标下颗粒的速度、温度等参数; 计算相间源项。

5 双级透平内颗粒湍流扩散的 Lagarange 数值模拟

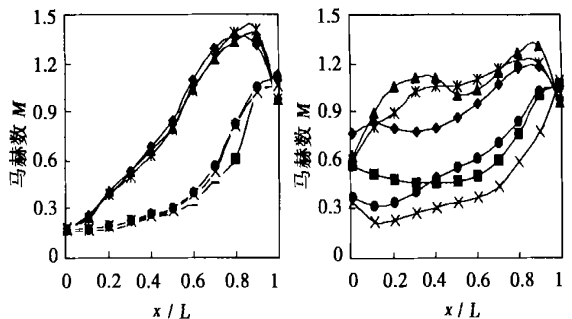
5.1 数值模拟结果与分析

在一双级燃气轮机透平内, 采用有限体积法离散基本方程, 以 SIMPLE 算法求解流场。每排叶片内按轴向、径向和周向共采用 $40 \times 20 \times 20$ 计算网格。透平按等内径设计, 静叶为直叶片, 动叶为扭叶片, 轮毂直径 700 mm, 汽缸壁的扩张角为 15° , 叶片的主要几何参数见表 1。初参数和主要热力参数为: 进口总压 0.594 3 MPa, 进口总温 1 033 K, 出口根部静压 0.104 4 MPa, 透平转速 7 800 r/min, 气体常数 281.53 m/(kg·K), 定压比热 1.203 3 kJ/(kg·K), 绝热焓降 414.43 kJ/kg, 比热比 1.308 9。

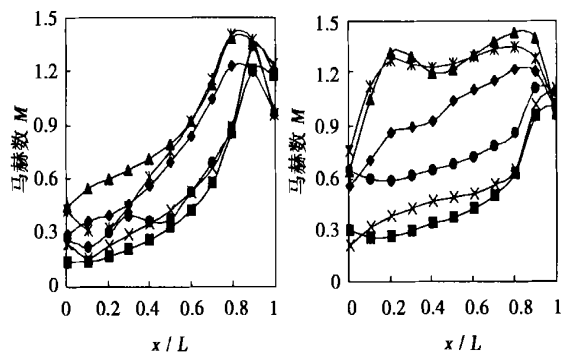
表 1 叶片排主要几何参数

叶片排序号	根部安装角/ $^\circ$	叶片出口高度/mm	叶片数
第一级静叶	39.0	70	49
第一级动叶	59.5	87	52
第二级静叶	43.0	105	49
第二级动叶	62.5	122	52

图 1(a)和(b)给出了叶片排内马赫数分布, 近吸力面和压力面的流体经历了由亚音速向超音速变化的过程, 叶片表面都有局部的超声速区域, 吸力面超声速区出现得较早, 而压力面的超声速区则出现近流道的出口, 更为详细的流场分析见文献 [7]。



(a) 第一级静叶和动叶马赫数 M 沿叶高的分布



(b) 第二级静叶和动叶马赫数 M 沿叶高的分布

◆ 叶顶吸力面 ■ 叶顶压力面 ▲ 中径吸力面
* 中径压力面 * 根径吸力面 ● 根径压力面

图 1 第一、二级静叶和动叶马赫数 M 沿叶高的分布

在此流场中, 先分别数值模拟粒径为 $5 \mu\text{m}, 10 \mu\text{m}, 25 \mu\text{m}, 50 \mu\text{m}, 150 \mu\text{m}$ 煤颗粒的湍流扩散运动轨迹。图 2 以第一列动叶入口为例, 说明了不同粒径颗粒与气相之间的速度滑移程度。由于颗粒密度较气体大得多, 颗粒与气体之间的运动滑移随粒径的增大而明显加剧。

图 3(a)、图 4(a)、图 5(a)和图 6(a)均采用本文模型得到的模拟结果。 $5 \sim 10 \mu\text{m}$ 小粒径颗粒在耦合后脉动流场触发下, 同时向叶根和叶顶运动, 颗粒运动轨迹沿叶高呈相对均匀的态势。叶片入口处, 栅距两侧的颗粒首先撞击叶片压力面和吸力面的进气边, 在反弹过程中, 被气流裹带流向下流, 碰撞叶片其它部位的机会很少。

$25 \mu\text{m}$ 以上的颗粒相对于气流开始呈运动滑移, 颗粒撞击叶片进气边后开始反弹, 未撞击进气

边的颗粒由于惯性可能直接冲击压力面的中部和出气边, 再经反弹后流向下游。沿径向, 耦合后的湍流场对颗粒仍有较大影响, 表现在颗粒轨迹沿叶高的分布显现一定的随机性。

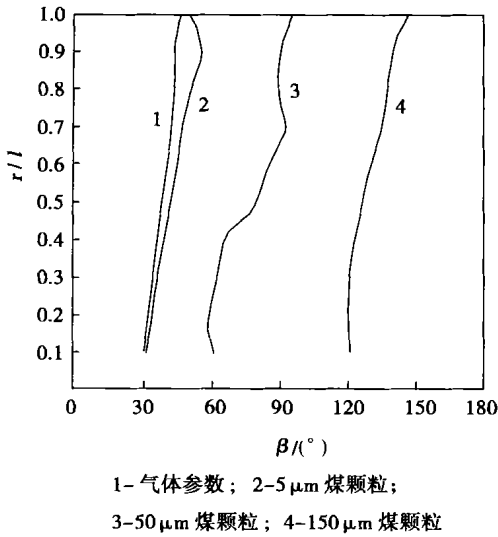


图 2 第一列动叶入口处颗粒速度滑移情况

50 μm 的颗粒已具较大惯性, 以第一列动叶入口为例, 颗粒进入叶片时, 对进气边产生激烈冲击, 导致在流道内接二连三地反弹而冲击叶片的压力面和吸力面, 形成压力面中部及出气边区域严重的冲蚀。数值模拟中发现, 后面叶片排内颗粒总数有所减少, 说明一部分颗粒由于动能损失未到叶片出口便向叶根沉降。

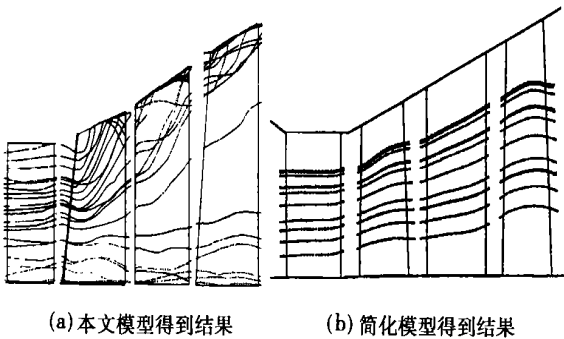


图 3 $d=5 \mu\text{m}$ 颗粒在流道中的运动轨迹

图 3(b)、图 4(b)、图 5(b)和图 6(b)是在简化模型条件下的模拟结果。由于仅考虑气相对颗粒的作用(单向耦合), 又忽略了颗粒的湍流扩散, 颗粒主要在离心力的作用下过分夸张地偏向叶顶(不计重力时更是如此)。一方面, 5 ~ 50 μm 的颗粒从第二排

叶片起就开始偏离叶根流动, 没有如实地反映小颗粒在叶片根部的运动特点及对叶片的磨损, 因此很难解释气固两相透平中叶片根部为何存在严重的二次磨损和型线破坏; 另一方面, 图 3(b)和图 4(b)中 5 ~ 10 μm 颗粒又没有到达叶顶, 似乎这些颗粒不会构成动叶叶尖的冲蚀磨损, 这与 PFBC 燃气透平(三级分离后, 主要含小颗粒)叶片顶部的实际磨损情况又是不相符合的, 主要原因是忽略了湍流扩散。

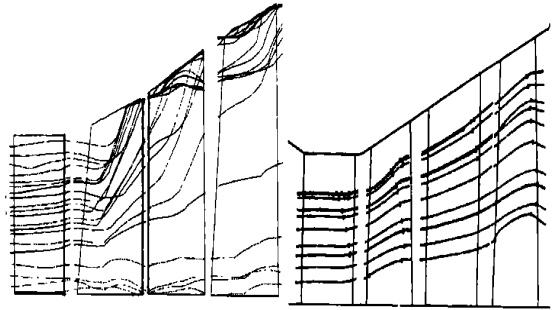


图 4 $d=10 \mu\text{m}$ 颗粒在流道中的运动轨迹

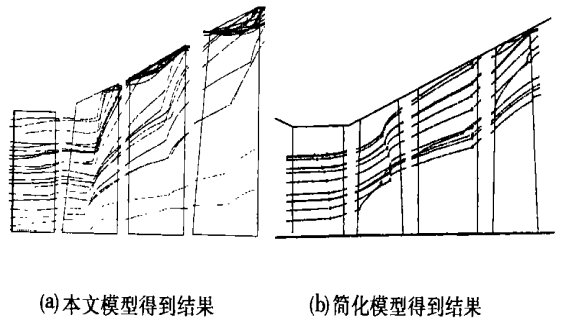


图 5 $d=25 \mu\text{m}$ 颗粒在流道中的运动轨迹

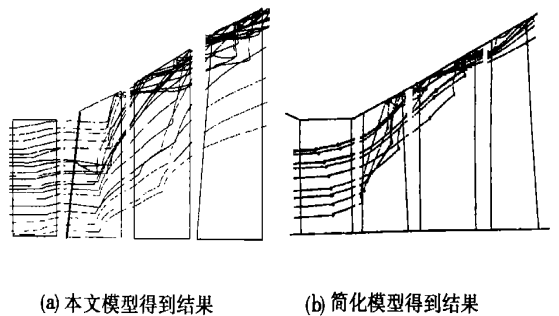


图 6 $d=50 \mu\text{m}$ 颗粒在流道中的运动轨迹

在透平的入口, 又给定了 10 万颗 5 ~ 50 μm(颗粒体积分数 $0.903 \times 10^{-4} \%$) 满足分布规律的煤颗

粒,数值模拟了4个叶片排内混合颗粒的湍流扩散运动以及与叶片的碰撞。在叶片根部、顶部和压力面得到了与实际叶片冲蚀点分布较为吻合的颗粒轨迹(如图7和图8),表明采用颗粒湍流扩散的Lagarange数值模拟方法确能取得较满意的结果。

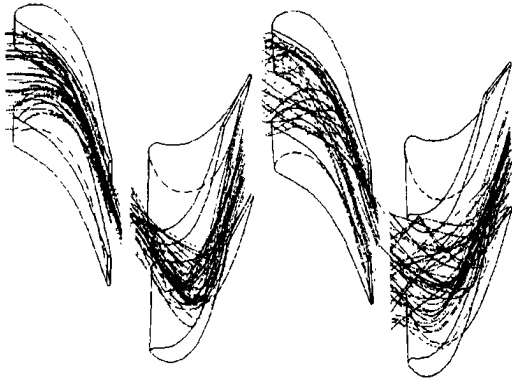


图7 叶片排内5~50 μm颗粒的运动轨迹

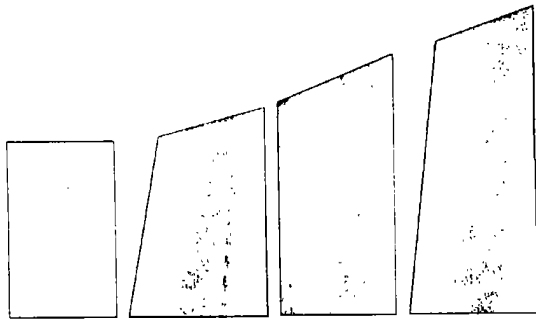


图8 5~50 μm煤颗粒在叶片排压力面上的碰撞点分布(体积分数 $0.903 \times 10^{-4} \%$)

5.2 激波对颗粒运动的影响分析

表2是叶片排内颗粒与叶片碰撞的信息统计。透平叶片压力面的出气边附近,是颗粒碰撞最严重的部位,直接的原因是颗粒于进气边处首先碰撞叶片吸力面后经反弹至压力面出气边,以较快速度对该部位再次碰撞所致,而近出气边吸力面上却没有颗粒与叶片碰撞。较为合理的解释是颗粒在吸力面近出气边处遭遇了激波的干扰,在与叶片碰撞之前,颗粒运动的动量不足以克服较强的波阻而发生运动的偏转。由于叶片出气边处,激波强度沿周向由吸力面向压力面方向减弱,故颗粒的偏转方向由原先贴近吸力面而转向波阻较小的流道中心。同时又由于激波沿叶高存在,颗粒的偏转现象就沿整个

叶高上发生,所以沿径向,吸力面近出气边处几乎无颗粒冲蚀叶片。

表2 各叶片排近出气边处颗粒碰撞叶片的信息

叶片排	压力面上 颗粒数	平均冲 角/(°)	平均冲蚀 速度/ $m \cdot s^{-1}$	吸力面上 颗粒数	平均冲 角/(°)	平均冲蚀 速度/ $m \cdot s^{-1}$
第一级静叶	18 192	36.97	191.04	0	—	—
第一级动叶	67 896	23.89	233.92	0	—	—
第二级静叶	22 390	27.75	227.03	0	—	—
第二级动叶	43 795	20.59	218.15	0	—	—

6 结束语

经过分离以后进入透平的微细颗粒弛豫时间极短,在脉动速度场的作用下颗粒湍流扩散运动的特征得以充分显现。颗粒由于较大的重度在叶片流道内的运动惯性与气体之间形成了明显的运动滑移,两相流体的相对运动凸现了黏性的影响。因此两相流体间的渗混必须予以考虑。本文的模型综合考虑了气固两相之间的动量、湍动能以及湍动能耗散的双向耦合,与简化模型的模拟结果比较,叶片流道内颗粒湍流扩散的Lagarange运动数值模拟结果与实际叶片受颗粒撞击的分布情况更为吻合,说明在黏性流场下采用气固双向耦合的颗粒随机轨道模型数值模拟叶片流道内颗粒湍流扩散运动是有成效的,其意义在于能为优化气固两相透平叶片的气动设计提供更可靠的依据。

参考文献:

- [1] 姜小敏,凌志光,邓兴勇.含尘流透平叶片冲蚀的数值分析[J].工程热物理学报,2000,22(1):60-62.
- [2] TABAKOFF W, METWALLY M. Coating effect on particle trajectories and turbine blade erosion[J]. *J of Engineering for Gas Turbine and Power*, 1992, 114(2): 250-257.
- [3] HIROYUKI TASHIRO, EIJI WATANABE, HITOSHI SHINANO, et al. Effect of mixing gas-fine particle suspension flow with small amount of coarse ones in a horizontal pipe[J]. *Int J Multiphase Flow*, 2001, 27(3): 2001-2013.
- [4] BERLEMONT A, DESJONQUERES P, GOUESBET G. Particle lagrangian simulation in turbulent flows[J]. *Int J Multiphase Flow*, 1990, 16(1): 19-34.
- [5] 陆宏圻.流体机械与流体动力工程[M].武汉:武汉水利大学出版社,1998.
- [6] 鲁嘉华.黏性流场下透平机械叶片冲蚀的数值模拟与试验研究[D].上海:上海理工大学,2002.
- [7] 鲁嘉华,凌志光.某双级跨音速燃气透平全三元黏性流场的数值分析[J].能源技术,2001,22(4):141-145.

(渠 源 编 辑)

变频调速技术的发展及其在电力系统中的应用 = **Development of Frequency Conversion-based Speed Governing Technology and Its Application in Electric Power Systems** [刊, 汉] / ZHANG Cheng-hui, CHENG Jin, XIA Dong-wei, et al (Institute of Control Science & Engineering under the Shandong University, Jinan, China, Post Code: 250061) // Journal of Engineering for Thermal Energy & Power. — 2003, 18(5). — 439 ~ 444

An overview of the development history and present status of frequency conversion-based speed governing technology is given from the standpoint of the use of electric power semiconductors, control technology and main circuit topology structures, etc. The main control techniques of the above-cited speed governing method are concisely described. An analysis is given of the development dynamics of high-voltage frequency conversion-based speed governing technology with the technical features of its several schemes now in use being compared. On the basis of the above the development tendency of the speed governing technology under discussion is outlined. In conclusion, its application aimed at energy conservation, technology and control performance enhancement is described. **Key words:** frequency conversion-based speed governing technology, vector control, AC motor, PWM (pulse width modification) technology, electric power system

煤粉燃烧一维温度分布可视化模拟研究 = **Simulation Study on the Visualization of One-dimensional Temperature Profiles in a Pulverized Coal-fired Boiler Furnace** [刊, 汉] / LI Li, JIANG Zhi-wei, LOU Chun, et al (State Key Laboratory on Coal Combustion under the Huazhong University of Science & Technology, Wuhan, China, Post Code: 430074) // Journal of Engineering for Thermal Energy & Power. — 2003, 18(5). — 445 ~ 449

Infrared thermal image devices currently available can only provide accumulative temperature images of a flame during the monitoring of the latter without the ability to present any information concerning the inner temperature distribution of the flame. Under certain conditions the local combustion process specific to a pulverized coal-fired boiler furnace can be approximated to a one-dimensional object. By using two probes for taking the picture of flame images respectively from two openings on a furnace wall and through the adoption of image processing techniques and radiation transmission principles a one-dimensional temperature distribution can be reconstructed between the two probes. With respect to two kinds of typical temperature profile and by the use of two kinds of flame monitoring mode a simulation study for each kind was respectively conducted. The simulation results indicate that a good reproduction effect of the temperature profiles can be achieved if flame detectors are mounted at an appropriate picture-taking angle, thus testifying to the significant usefulness of the method proposed by the authors. **Key words:** pulverized coal combustion, reconstruction of a temperature field, flame image processing

炉内煤粉燃烧一维数学模型及其仿真 = **One-dimensional Mathematical Model and Relevant Simulation for Pulverized Coal Combustion in a Boiler Furnace** [刊, 汉] / ZHANG Teng-fei, LUO Rui, REN Ting-jin, et al (Thermal Engineering Department, Tsinghua University, Beijing, China, Post Code: 100084) // Journal of Engineering for Thermal Energy & Power. — 2003, 18(5). — 450 ~ 453

The combustion mechanism of pulverized coal particles was studied with pulverized-coal burning process in the most complex combustion zone of a furnace serving an object of research. On this basis a one-dimensional macroscopic model featuring pulverized coal combustion along the furnace height was set up to accurately calculate the burn-off rate of the pulverized coal in the furnace. Through a rational simplification of the combustion process of volatile matter and coke in the pulverized coal the model has taken into account the variation of oxygen content during the pulverized-coal combustion. With the iso-density model of a single pulverized-coal particle combustion serving as a basis an integral process of pulverized coal combustion is reflected through the combustion process of pulverized coal of various particle diameters. Thus, a formula for calculating the burn-off rate of pulverized coal in a furnace has been developed, meeting the requirements of real-time simulation computations. The results of simulation calculations are analyzed and found to be in good agreement with measured data and those given in current literature. **Key words:** pulverized coal combustion, isodensity model, macroscopic model, real-time simulation

气固两相透平内颗粒湍流扩散的 Lagrange 数值模拟 = **Lagrangian Numerical Simulation of Particle Turbulent**

Diffusion in a Gas-solid Two-phase Turbine [刊, 汉] / LU Jia-hua, LING Zhi-guang (College of Aviation Transportation under the Shanghai University of Engineering & Technology, Shanghai, China, Post Code: 200336) // Journal of Engineering for Thermal Energy & Power. — 2003, 18(5). — 454 ~ 458

In the totally three-dimensional viscous turbulent flow field of a dual-stage transonic gas turbine a Lagrangian numerical simulation was respectively conducted of the turbulent diffusion movement of coal particles of different particle sizes and mixed coal particles of 5—50 μm distribution diameter (volume fraction = $0.903 \times 10^{-4}\%$) in a blade flow path. This was accomplished with the use of a gas-solid two-way coupled model. As a result, the corresponding movement trajectories and slippage were obtained. As compared to the results of numerical simulation under the assumed condition of non-viscid, laminar flow and one-direction coupling, more realistic movement characteristics of particles were secured. It should be specially noted that at the blade pressure surface, blade root and tip the distribution of impact-point of particles with blades is in relatively good agreement with the distribution condition of actual blade impact/erosion points. This has confirmed the non-negligible effect of the turbulent diffusion characteristics of particles in the blade flow path. The results of the numerical simulation will provide a more reliable basis for furthering the optimization of the aerodynamic design of gas-solid two-phase turbine blades. **Key words:** gas-solid two-phase turbine, viscous turbulent flow field, turbulent diffusion, two-way coupling, Lagrangian method, numerical simulation

修正的 $k-\epsilon-k_p$ 双流体模型用于模拟旋流突扩燃烧室内气固两相流动 = Numerical Simulation of Gas-solid Two-phase Flows in a Swirling-flow Combustor through the Use of a Modified $k-\epsilon-k_p$ Two-fluid Model [刊, 汉] / LI Zhi-qiang, WEI Fei, LI Rong-xian, et al (Department of Chemical Engineering, Tsinghua University, Beijing, China, Post Code: 100084) // Journal of Engineering for Thermal Energy & Power. — 2003, 18(5). — 459 ~ 462

The source item of ϵ equation in a standard $k-\epsilon-k_p$ model after a modification is used to simulate swirling gas-solid two-phase turbulent flows. The simulation results were compared with experimental data. The resulting modified model can relatively well simulate the swirling flows and play a significant role in promoting an optimized engineering design. **Key words:** swirling flow, modified $k-\epsilon-k_p$, two-fluid model, numerical simulation

有再循环系统的超音速两相流升压性能的研究 = A Study on the Performance of a Supersonic Steam-liquid Two-phase Flow Pressure-boosting Unit Equipped with a Hot-water Recirculation System [刊, 汉] / GUO Ying-li, LI sheng, YAN Jun-jie, et al (College of Energy and Power Engineering under the Xi'an Jiaotong University, Xi'an, China, Post Code: 710049) // Journal of Engineering for Thermal Energy & Power. — 2003, 18(5). — 463 ~ 466

A theoretical calculation and experimental study is conducted of a supersonic steam-liquid two-phase flow pressure-boosting unit, which incorporates a hot-water recirculation system. It has been found that under a condition of constant inlet steam parameters the pressure boosting performance will decrease with an increase in feed water temperature and increase with an increase in outlet water flow. The outlet water temperature will decrease with an increase in outlet water flow, and increase with a rise in feedwater temperature. The unit under discussion not only retains the self-adaptive characteristics of the original outlet pressure, but also features self-adaptive characteristics of outlet flow rate. **Key words:** supersonic, steam-liquid two-phase flow, shock wave, constant flow rate characteristics

一种湿法烟气脱硫方式的试验研究 = Experimental Research of a Wet-process Flue-gas Desulfurization Method [刊, 汉] / SAI Jin-Cong, WU Shao-hua, WANG Hong-tao (College of Energy Science & Engineering under the Harbin Institute of Technology, Harbin, China, Post Code: 150001) // Journal of Engineering for Thermal Energy & Power. — 2003, 18(5). — 467 ~ 470

A flue gas desulfurization method based on the use of a groove-shaped flow-guide core and flue-gas transverse sweep is proposed, which has been studied on a small-size test rig. A qualitative analysis was conducted of the impact of flue gas flow speed, temperature and gas-liquid contact area on flue-gas desulfurization efficiency. The slag formation problem of the test rig is also briefly analyzed and discussed. **Key words:** transverse sweep of gases, groove-type core, wet-process flue-gas desulfurization, slag formation